2014

Regional brain metabolism in a murine systemic lupus erythematosus model

An Vo
Hofstra Northwell School of Medicine

B. T. Volpe
Hofstra Northwell School of Medicine

C. C. Tang
Northwell Health

W. K. Schiffer
Northwell Health

C. Kowal
Northwell Health

See next page for additional authors

Authors
An Vo, B. T. Volpe, C. C. Tang, W. K. Schiffer, C. Kowal, P. T. Huerta, A. M. Ulug, S. L. Dewey, D. Eidelberg, and B. Diamond

OPEN

Journal of Cerebral Blood Flow & Metabolism (2014) 34, 1315–1320

www.jcbfm.com

ORIGINAL ARTICLE

Regional brain metabolism in a murine systemic lupus erythematosus model

An Vo[1,4], Bruce T Volpe[2,4], Chris C Tang[1,4], Wynne K Schiffer[1,4], Czeslawa Kowal[2], Patricio T Huerta[3], Aziz M Uluğ[1], Stephen L Dewey[1], David Eidelberg[1,5] and Betty Diamond[2,5]

Systemic lupus erythematosus (SLE) is characterized by multiorgan inflammation, neuropsychiatric disorders (NPSLE), and anti-nuclear antibodies. We previously identified a subset of anti-DNA antibodies (DNRAb) cross-reactive with the *N*-methyl-D-aspartate receptor, present in 30% to 40% of patients, able to enhance excitatory post-synaptic potentials and trigger neuronal apoptosis. DNRAb + mice exhibit memory impairment or altered fear response, depending on whether the antibody penetrates the hippocampus or amygdala. Here, we used 18F-fluorodeoxyglucose (FDG) microPET to plot changes in brain metabolism after regional blood–brain barrier (BBB) breach. In DNRAb + mice, metabolism declined at the site of BBB breach in the first 2 weeks and increased over the next 2 weeks. In contrast, DNRAb − mice exhibited metabolic increases in these regions over the 4 weeks after the insult. Memory impairment was present in DNRAb + animals with hippocampal BBB breach and altered fear conditioning in DNRAb + mice with amygdala BBB breach. In DNRAb + mice, we observed an inverse relationship between neuron number and regional metabolism, while a positive correlation was observed in DNRAb − mice. These findings suggest that local metabolic alterations in this model take place through different mechanisms with distinct time courses, with important implications for the interpretation of imaging data in SLE subjects.

Journal of Cerebral Blood Flow & Metabolism (2014) **34,** 1315–1320; doi:10.1038/jcbfm.2014.85; published online 14 May 2014

Keywords: autoantibodies; behavior; FDG-microPET; *N*-methyl-D-aspartate receptor; stereological neuron count

INTRODUCTION

Systemic lupus erythematosus (SLE) is an autoimmune disease characterized by autoantibodies to nuclear antigens and systemic inflammation. Anti-DNA antibodies are the most common autoantibody, and cognitive and behavioral impairments are common central nervous system (CNS) symptoms.[1] Indeed, in the past few decades investigators have come to realize both the frequency and severity of the CNS manifestations of SLE in patients and in mouse models. Because the symptoms of CNS lupus are variable, and because brain tissue is rarely available for analysis premortem, an understanding of pathogenetic mechanisms of CNS manifestations of lupus, a major component of neuropsychiatric lupus (NPSLE), has proven difficult to achieve.

The pathophysiology for NPSLE in the CNS includes vascular and parenchymal damage.[2] Focal lesions result from inflammation or thrombosis in the vessels, often mediated by anti-phospholipid antibodies. The pathophysiology of diffuse CNS alterations is complex and includes insults not only from anti-neuronal antibodies, but probably also from cytokines and other inflammatory mediators.[1] Therefore, neuroimaging modalities have been employed to identify physiologic changes associated with NPSLE.[3]

Functional brain imaging studies conducted in patients with SLE have produced inconsistent findings. ^{18}F-fluorodeoxyglucose (FDG) PET, which assays regional brain glucose utilization, has revealed multifocal reductions in the frontal, parietal, and temporal gray matter,[4–9] changes thought to represent underlying cell injury, neuronal death, or a combination of the two. However, the observed metabolic changes seldom correlate with the localization or severity of symptoms. More recent investigations have shown increased glucose metabolism localized to the white matter, consistent with the white matter loss in structural imaging studies.[7,10–13] Indeed, these changes have been thought to reflect non-neuronal glucose metabolism and inflammation,[12,14] and to precede the development of gray matter hypometabolism secondary to deafferentation or neuronal loss, or both.

To understand the basis for these disparate findings, we have developed an animal model with a defined time of onset and mechanism of brain injury. Because autoantibodies are a major trigger for tissue injury in inflamed organs in SLE, we have focused on brain-reactive antibodies. Anti-neuronal antibodies were demonstrated in SLE patients many years ago, but a lack of identification of the antigenic target impeded mechanistic insight into their potential pathogenicity. We demonstrated that a subset of anti-DNA antibodies (DNRAb) also binds the *N*-methyl-D-aspartate receptor (NMDAR).[15,16] These antibodies can be generated experimentally in mice.[17,18] The antibodies preferentially bind the active receptor and augment the effects of glutamate, enhancing excitatory post-synaptic potentials, and inducing excitotoxic neuron death at high concentrations.[19] Treatment of DNRAb + mice with an insult to the BBB in the

[1]Center for Neurosciences, The Feinstein Institute for Medical Research, Manhasset, New York, USA; [2]Center for Autoimmune and Musculoskeletal Disease, The Feinstein Institute for Medical Research, Manhasset, New York, USA and [3]Laboratory of Immune & Neural Networks, The Feinstein Institute for Medical Research, Manhasset, New York, USA. Correspondence: Dr B Diamond, Center for Autoimmune and Musculoskeletal Disease, The Feinstein Institute for Medical Research, 350 Community Drive, Manhasset, NY 11030, USA.

E-mail: bdiamond@nshs.edu

[4]These authors contributed equally to this work.

[5]Co-senior authors.

Received 11 March 2014; revised 16 April 2014; accepted 22 April 2014; published online 14 May 2014

hippocampus leads to an ensuing memory impairment,[17] while compromised BBB function in the amygdala leads to an alteration in an associatively learned fear response.[20] The initial lesion in both situations is neuron loss within the region exposed to DNRAbs without infiltration of blood–borne inflammatory cells into the brain tissue. In this study, we used serial FDG-microPET to define the regional distribution and time course of the alterations in brain metabolism that result from lipopolysaccharide (LPS) or epinephrine-induced exposure to DNRAbs. By assessing metabolic activity at baseline, and twice more after the BBB insult, we found comparable changes in metabolism that occurred in DNRAb exposed regions. We also found metabolic changes that were specifically related to local BBB breach, independent of DNRAb exposure.

MATERIALS AND METHODS

Animals, Immunization Protocol, Enzyme-Linked Immunosorbent Assay and Lipopolysaccharide or Epinephrine Treatment

Animals were handled according to the NIH Guide for the Care and Use of Laboratory Animals and all procedures were approved by the IACUC at the Feinstein Institute. Six- to eight-week-old BALB/c female mice from the Jackson Laboratory (Bar Harbor, ME, USA) were used in all experiments. The immunization protocols have been published.[17] Briefly, 20 mice were immunized by intraperitoneal injection with 100 μg of antigen, either MAP-DWEYS ($n = 10$) or MAP-core (polylysine backbone) ($n = 10$) (AnaSpec, San Jose, CA, USA) in complete Freund's adjuvant followed by two boosts (2-week intervals) in incomplete Freund's adjuvant. Enzyme-linked immunosorbent assays were performed after each immunization, as described previously.[18] Some immunized mice received an intraperitoneal injection of LPS (*Escherichia coli*, 055:B5, Sigma, St Louis, MO, USA) at a dose of 3 mg/kg diluted in lactated Ringer's solution to 0.3 mg/ml. Lipopolysaccharide treatments were given twice, 48 hours apart, at 4 weeks after the last immunization. Other mice received an intraperitoneal injection of epinephrine (100 nmol/L in Ringer's solution).[20]

Positron Emission Tomography Study in Mice

Animals received FDG (1.2–2.2 mCi/kg) intraperitoneally and moved freely in their home cage during the 45-minute uptake period, as described elsewhere.[21,22] Afterwards, animals were anesthetized with isoflurane, placed into a stereotaxic frame, and moved into the gantry for imaging. Animals were scanned at baseline (T1) before immunization with MAP-DWEYS or control MAP-core on the Siemens Inveon (Siemens AG, Munich, Germany) at the Feinstein Institute. They underwent repeat scanning at 2 (T2) and 4 weeks (T3) after LPS injection. For each scan, a single 10-minute static emission scan was obtained, followed by an 8-minute attenuation scan. Whole blood glucose values were collected in each scan and the animals were returned to their home cage. All images were corrected for attenuation and reconstructed using an iterative reconstruction approach (maximum *a priori* (MAP) algorithms), as well as standard filtered back projection algorithms. Using PMOD software (PMOD Technologies, Zurich, Switzerland), images were co-registered to a standard magnetic resonance imaging mouse atlas.[23] Serial metabolic data from DNRAb+ and DNRAb− mice were analyzed using statistical parametric mapping mouse software (http://www.wbic.cam.ac.uk/~sjs80/spmmouse.html),[24] as described elsewhere.[25,26] We first specified a hypothesis-testing mask, defined by the difference between the first (T1) and last (T3) time point scans acquired in the DNRAb− animals. The resulting mask was thresholded at $P = 0.001$ at peak voxel, and corrected for multiple comparisons at $P < 0.05$ (false-positive discovery rate). Significant group × time interaction effects on regional metabolism were sought within this space using the baseline (T1) and final (T3) scans from both groups of animals. We performed additional statistical parametric mapping analyses to evaluate group differences in the initial post -LPS time course (i.e., between T1 and T2), and to identify interaction effects across all three time points. For each analysis, clusters were considered significant for $P < 0.01$ (uncorrected), with a cluster-size cutoff of 200 voxels. To evaluate the time course of these effects, VOIs corresponding to significant regions were placed on the individual scans acquired at each time point. For each VOI, longitudinal changes in globally normalized metabolic activity were compared between groups using repeated measures analysis of variance with *post hoc* Bonferroni tests. Results were considered significant for $P < 0.05$.

Spatial Memory and Fear-Conditioning Task

Mice given LPS were assessed for spatial memory after the final PET scan was performed, at 8 weeks post-LPS administration. We used a navigational test (clock maze task)[16] that was modified from Deacon & Rawlins.[27] Mice given epinephrine were assessed for performance in a fear-conditioning paradigm.[20] Unmanipulated BALB/c mice were also studied in each task ($n = 10$ for the spatial memory task; $n = 9$ for the fear-conditioning task).

Brain Histology

Three mice in each group receiving LPS were killed after the third FDG-micro PET scan and cognitive testing, and their brains were perfused with heparinized saline followed by 4% paraformaldehyde, removed from the skull, and frozen in OCT. Brains were then cut so that every third 20-μm section through the dorsal anterior hippocampus and amygdala (bregma, −2.0 mm), the dorsal subiculum (bregma, −3.5 mm), and the ventral subiculum (bregma, −4.5 mm) could be sampled with fixed periodicity on a Leica microtome (Buffalo Grove, IL, USA). Coronal sections were stained with cresyl violet. Unbiased stereological neuron counts using cresyl violet or neuron specific neu-N stain has yielded comparable data in our database. Mosaic images of the regions of interest were compiled at × 100 oil (fixed total area = 0.044 mm2) in Z-stack arrangements (1-μm steps; Axio-Imager Z1, Zeiss, Thornwood, NY, USA). Images were analyzed using unbiased stereological techniques (Stereologer, MBF, Williston, VT, USA). A trained investigator (BTV), who was masked to the identity, experimental status, and imaging findings of the individual animals conducted the measurements. The coefficient of error for the stereological measurements across all the animals and all regions was, on average, 0.07 ($n = 60$). The histologic coordinates for estimating neuron number in the ventral subiculum were derived from the systematic sampling strategy and were within the region of PET activation, as PET regions of interest coordinates can be translated to standard atlas coordinates.[23] The sample histologic volume is ~1/50th the volume of the PET activated regions of interest.

Statistical Analysis

Repeated measures analysis of variance (RMANOVA), followed by *post hoc* Bonferroni tests, was used to examine the longitudinal changes in regional metabolism in the hippocampus or amygdala between the DNRAb+ and DNRAb− mice after the injection of LPS or epinephrine. Analysis of variance was also used to examine the changes in the performance in a clock maze memory task, and *t*-test was used to examine the performance in the tone and context fear conditioning. Nonparametric Mann–Whitney *U*-test was used to compare the number of neurons in the hippocampus between the DNRAb+ and DNRAb− mice. Nonparametric Spearman's correlation coefficient was calculated between the neuron number in the ventral subiculum and the metabolism in the corresponding regional cluster at 4 weeks post LPS for the DNRAb+ and DNRAb− animals. Statistical analyses were performed in SPSS 14.0 for Windows (SPSS, Chicago, IL, USA) or OriginPro 9.1 (OriginLabs, Northampton, MA, USA). Results were considered significant for $P < 0.05$.

RESULTS

In order to study the time course of behavioral, metabolic, and histopathological changes after hippocampal exposure to DNRAbs, mice were immunized with a peptide mimetope of DNA multimerized on a polylysine backbone to generate DNRAbs (DNRAb+ mice), or with the polylysine backbone alone (DNRAb− mice). Both mouse cohorts received LPS to breach the BBB in the hippocampus,[16,17,20] and underwent microPET at three time points: 1 week before LPS injection, and 2 weeks and 4 weeks after LPS administration.

A whole brain voxel-wise search was conducted to identify brain regions in which the time course of local metabolic activity differed for DNRAb+ and DNRAb− animals. This strictly data-driven analysis revealed only a single region, the ventral subiculum (Figure 1A) where a significant difference was found between the two groups of animals ($P = 0.01$; overall analysis

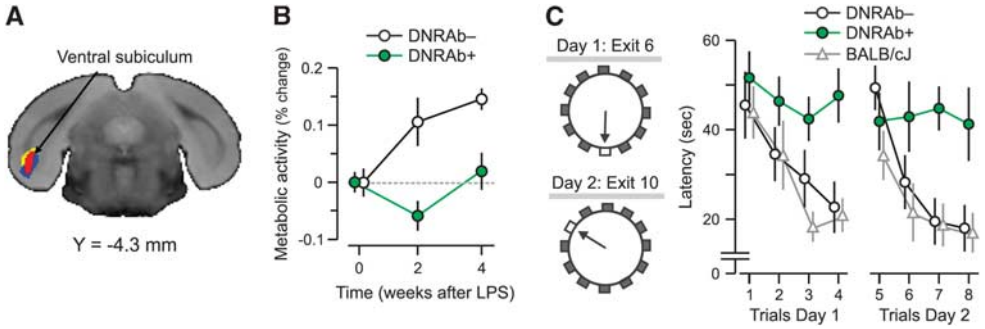

Figure 1. Panel **A** shows a voxel-based comparison of ^{18}F-fluorodeoxyglucose positron emission tomography images for mice carrying DNRAbs and controls. The strictly data-driven comparison of mice carrying DRNAbs (DNRAb+) and control (DNRAb−) mice reveals a single cluster in the ventral subiculum and entorhinal cortex (red) in which the metabolic changes significantly differ for the two groups over time. The red cluster in panel **A** was obtained by a statistical parametric mapping interaction analysis of two groups × two time points (0, 4 weeks) (voxel-wise $P \leqslant 0.01$, $k \geqslant 220$, cluster corrected $P < 0.05$). The yellow cluster was obtained by a statistical parametric mapping interaction analysis of two groups × three time points (0, 2, 4 weeks) (voxel-wise $P < 0.005$, $k > 500$, cluster corrected $P < 0.05$). The blue cluster was obtained by a statistical parametric mapping comparison of 0 and 2 weeks for the DNRAb+ mice (voxel-wise $P < 0.001$, $k > 640$, cluster corrected $P < 0.05$). The significant clusters from these three analyses were located in the ventral subiculum and entorhinal hippocampus and overlapped in this region. (**B**) Before LPS administration at baseline (0 weeks), resting metabolism in this region is equivalent in the DNRAb− (circles) and DNRAb+ (triangles) groups. The DNRAb+ mice show decreased regional metabolism 2 weeks after LPS administration that is reversed by 4 weeks after LPS injection. In contrast, the DNRAb− mice demonstrate continuously increasing regional metabolism from 0 weeks through 2 and 4 weeks. Of note, the rate of metabolic increase between 2 and 4 weeks was relatively faster in DNRAb+ mice (0.4/week) than for DNRAb− mice (0.2/week). There was a significant difference in the metabolic changes between the two groups over time (group × time interaction effect: $F[2,36] = 4.8$, $P = 0.01$; two-way repeated measures analysis of variance (RMANOVA) on the data at all three time points). Further analyses revealed that this interaction effect occurred in the first 2 weeks after the injection (group × time interaction effect: $F[1,18] = 6.73$, $P = 0.02$; two-way RMANOVA on the data at baseline and 2 weeks), but not over the subsequent 2 weeks (group × time interaction effect: $F[1,18] = 0.44$, $P = 0.52$; two-way RMANOVA on the data at 2 and 4 weeks). (**C**) DNRAb+ mice ($n = 10$) and DNRAb− controls ($n = 10$) were tested in the clock maze task 8 weeks post-LPS administration. DNRAb+ mice had impaired spatial memory $F[2,7] = 6.8$, $P = 0.02$, analysis of variance). A cohort of unmanipulated BALB/c mice was also tested. There was no difference between this cohort and the DNRAb− mice.

three time points). The significant interaction occurred in the first 2 weeks ($P = 0.01$) but not in the subsequent 2 weeks ($P = 0.52$). (Figure 1B).

No difference in the time course of global metabolic activity after LPS was present between the two groups ($P = 0.57$). Globally normalized metabolic activity in the ventral subiculum rose steadily in the DNRAb− animals over the 4 weeks that followed LPS administration. In contrast, changes seen in the DNRAb+ group after LPS administration had a significantly different time course ($P = 0.01$). These animals exhibited a decline in the metabolic activity in this region between baseline and the 2-week post-LPS time point, followed by an increase in metabolic activity at 4 weeks post LPS. The profile was consistent with a biphasic process, in which the initial DNRAb-mediated insult in the area of BBB breach led to a decreased metabolism presumably secondary to neuronal loss, which we have previously shown occurs in the first week after antibody exposure.[17] This first phase was followed by a phase of increasing metabolism that may represent local glial cell inflammation, a compensatory neuronal metabolic response, or a combination of the two.

After microPET, the LPS-treated mice were subjected to memory assessment, with the investigator masked to the treatment group. DNRAb+ mice ($n = 9$) were impaired compared to DNRAb− mice in spatial memory ($P = 0.02$) when tested in a clock maze at 8 weeks post LPS[17] (Figure 1C). There was no detectable difference between DNRAb− mice and the unmanipulated BALB/c mice (Figure 1C).

Histopathological analysis with unbiased stereology was obtained in the dorsal CA1 and CA3 fields of the hippocampus, ventral subiculum, posterior entorhinal cortex, and the lateral anterior dorsal and superior basal lateral amygdala. DNRAb+ mice ($N = 3$) displayed significant reductions in the number of neurons in the hippocampal regions previously shown to sustain neuron loss (the CA1, and also in the CA3, ventral subiculum and posterior entorhinal cortex) in comparison with DNRAb− mice ($N = 3$). Importantly, neuron number was also depressed in the ventral subiculum, a region that overlapped with the microPET data. Neuron number in the amygdala was comparable ($P = 1$) (Figure 2A). Correlations between cell number in the ventral subiculum and the metabolic activity in the corresponding regional cluster at 4 weeks post LPS (Figure 2B) differed for DNRAb+ and DNRAb− animals. DNRAb− mice exhibited a significant positive correlation between neuron number and metabolic activity (Figure 2B, open circles), contrasting with a negative correlation between neuron number and metabolic activity in this region in DNRAb+ mice (Figure 2B, green).

These findings support the hypothesis that the hippocampal metabolic reductions observed at 2 weeks post LPS in the DNRAb+ mice were a reflection of recent local neuron loss. The increases in metabolic activity that subsequently developed in these animals may represent a compensatory response of the surviving neurons in this brain region, a metabolic response in non-neuronal cells, or a combination of the two effects. The progressive metabolic increases in this region in DNRAb− mice at 2 and 4 weeks after hippocampal breach may represent an acute inflammatory response of glial cells to LPS exposure without the cognitive impairment observed after hippocampal exposure to DNRAbs.

To study the metabolic and behavioral changes after epinephrine in the SLE animal model, mice were immunized as before, but both DNRAb+ and DNRAb− cohorts received epinephrine (intrapertioneal 100 nmol/L epinephrine (Sigma)) in lactated Ringer's solution, as published, to breach the BBB in the amygdala, and underwent microPET at three time points: 1 week before LPS injection, and 2 weeks and 4 weeks after LPS administration.[16,17,20] We determined if analogous DNRAb-mediated changes in metabolism occurred in the amygdala after localized epinephrine-induced BBB breach. Mice underwent FDG-PET 1 week before epinephrine administration and 2 and 4 weeks later. There was no significant difference in the course of global

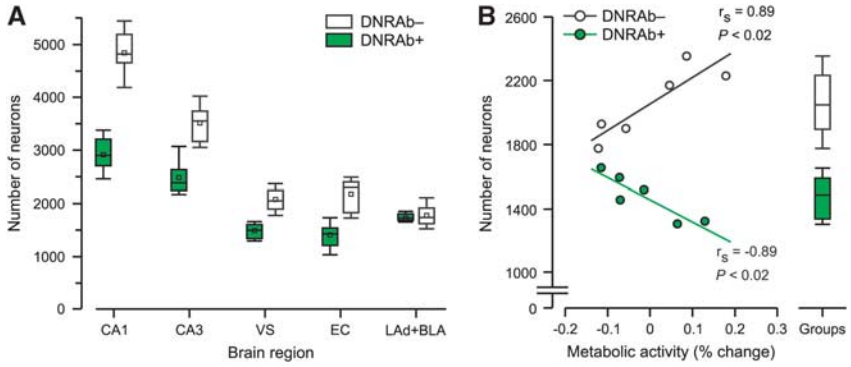

Figure 2. Panel **A** shows the number of neurons in the ventral subiculum in the DNRAb + mice was decreased ($P<0.005$) 4 weeks after bloor–brain barrier breach with lipopolysaccharide (LPS). This anatomic locus is comparable with the microPET loci. Neuron number in the hippocampal CA1, CA3 and entorhinal region was decreased in DNRAb + mice. Notably, the number of neurons in the amygdala (lateral amygdala (LAd) and superior basolateral amygdala) was comparable. Neuron number was measured from both hemispheres of three animals measured at 4 weeks for each group. Box-and-Whisker plots display the median and 25th and 75th percentiles of the neuron number of animals in both groups. DNRAb + mice had significant loss of neurons in the dorsal CA1 ($P<0.0001$), CA3 ($P<0.008$), ventral subiculum ($P<0.005$), and posterior entorhinal cortex ($P<0.005$; Mann–Whitney). Neuron number in the amygdala was comparable ($P=1$). (**B**) In DNRAb + mice (red), there was a significant inverse correlation ($P<0.02$) between the neuron number in the ventral subiculum and metabolism, suggesting a compensatory response of the neurons or glial cells to the DRNAb-mediated insult. In contrast, the DNRAb − mice (black) demonstrate a positive correlation ($P<0.02$) between neuron number in the ventral subiculum and metabolism.

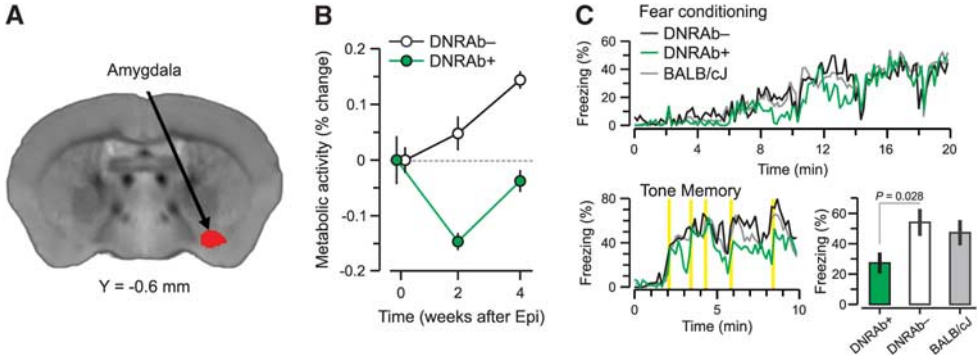

Figure 3. Panel **A** shows a voxel-based comparison of ^{18}F-fluorodeoxyglucose positron emission tomography images for mice carrying DNRAbs and controls. The strictly data-driven comparison of mice carrying DRNAbs (DNRAb +) and control (DNRAb −) mice reveals a single cluster in the amygdala (red) in which the metabolic changes significantly differ for the two groups over time. The red cluster in panel **A** was obtained by a statistical parametric mapping interaction analysis of two groups × two time points (0, 4 weeks) (voxel-wise $P<0.005$, $k>370$, cluster corrected $P<0.05$). (**B**) Before epinephrine administration at baseline (0 weeks), resting metabolism in this region is equivalent in the DNRAb − (circles) and DNRAb + (triangles) groups. The DNRAb + mice show decreased regional metabolism 2 weeks after epinephrine administration that is reversed by 4 weeks after epinephrine injection. In contrast, the DNRAb − mice demonstrate continuously increasing regional metabolism from 0 weeks through 2 and 4 weeks. Of note, the rate of metabolic increase between 2 and 4 weeks was relatively faster in DNRAb + mice (0.4/week) than for DNRAb − mice (0.2/week). There was a significant difference in the metabolic changes between the two groups over time (group × time interaction effect: F [2,36] = 9.59, $P\leqslant0.001$; two-way repeated measures analysis of variance (RMANOVA) on the data at all three time points). Furthermore, this interaction effect was present in the data at baseline and 2 weeks after the injection (group × time interaction effect: F[1,18] = 10.76, $P=0.005$; two-way RMANOVA), but was absent between 2 and 4 weeks (group × time interaction effect: F[1,18] = 0.10, $P=0.75$; two-way RMANOVA on the data at the last two time points). (**C**) Profile of freezing response. DNRAb + mice ($n=10$) and DNRAb − controls ($n=10$) were tested in an associative learning fear paradigm 8 weeks post-epinephrine administration. DNRAb + mice had impaired associative learning of the fear response in the tone memory test ($P=0.0007$, t-test). A cohort of unmanipulated BALB/c mice was also tested and their behavior was not different from the behavior of DNRAb − mice.

metabolism measured in the DNRAb + and DNRAb − groups over time ($P=0.12$). The DNRAb − mice exhibited a continuous increase in globally normalized metabolism in the amygdala across the three time points. In contrast, DNRAb + mice exhibited a metabolic decline in the amygdala at 2 weeks (Figure 3A), followed by increased activity in the same region at 4 weeks after epinephrine ($P\leqslant0.001$) (Figure 3B).

Behavior of both cohorts of mice was analyzed using a fear-conditioning paradigm. DNRAb + mice exhibited significantly decreased freezing scores compared to DNRAb − mice in the tone memory test ($P=0.007$), as previously demonstrated[20] (Figure 3C). As with LPS-treated DNRAb − mice, there was no impairment in the epinephrine-treated DNRAb − mice compared to unmanipulated BALB/c mice (Figure 3C).

DISCUSSION

This study demonstrates localized increases in metabolic activity in the hippocampus or amygdala after BBB disruption. Irrespective of the insult mediating BBB disruption and the location of BBB breach, DNRAb + mice exhibited a pattern of metabolic change that was not present in DNRAb − mice; local metabolic activity

was reduced relative to baseline at 2 weeks after BBB breach. Obviously, LPS and epinephrine may have regional effects beyond BBB breach, but the differential outcomes in the DNRAb+ and DNRAb− mice demonstrate the critical importance of barrier breach. Thus, reduced metabolic activity was transient and, therefore, would be unlikely to be detected as a consistent change in cross-sectional human studies. Crucially, an unbiased count of neurons within the hippocampal formation confirmed DNRAb-mediated neuron loss, consistent with our prior observation that neuronal death occurs in first week after DNRAb exposure.[17] Moreover, the inverse correlation in DNRAb+ mice between hippocampal cell counts and metabolic activity at the 4-week time point suggests the gradual development of a distinct and delayed tissue response. Blood–brain barrier integrity has been shown to be restored soon after LPS administration.[28] Our own data have demonstrated that no antibody is detectable in the hippocampus within days of the BBB breach. Thus, the increase in metabolism that occurs between 2 and 4 weeks after LPS administration reflects either classic compensation with metabolic increases that are 'normalizing' tissue activity, or a non-neuronal inflammatory mechanism (for example, a glial inflammatory response to neuronal necrosis) that raises metabolic activity, albeit from the depressed levels seen at 2 weeks. It will be important to know whether the increase continues beyond 4 weeks leading to greater than normal hippocampal metabolism in DNRAb+ mice. Further, microglial activity in DNRAb+ mice needs to be explored. By contrast, in DNRAb− animals, cell counts and metabolism in the hippocampal formation exhibit a positive correlation consistent with a localized inflammatory response of glial cells that does not impair memory. Thus, normal FDG metabolism may be observed in both healthy and damaged tissue, and similar metabolic profiles may associate with distinct neurobehavioral outcome assessments. This phenomenon of similar FDG-PET findings with distinct etiologies and behavioral consequences was observed also in the DNRAb+ mice with BBB breach in the amygdala. Finally, a compensatory increase in the hippocampal activity accords well with findings from functional magnetic resonance imaging activation studies in SLE patients.[29–32]

In summary, the data presented suggest a model for some NPSLE in which DNRAb-mediated cell loss in the hippocampus is associated with a compensatory response in the surviving neurons and subsequent increases in local glucose metabolism. However, a localized response to other potential insults in SLE can similarly result in abnormal metabolism in this region. Future studies should determine whether these two pathologic entities can be distinguished, and whether the increase in metabolism that begins at 2 weeks after LPS in DNRAb+ mice continues such that the mice eventually display increased hippocampal metabolism. We propose a combination of ^{11}C-PK11195 and ^{18}F-FDG-PET to measure microglial activation and regional metabolism to provide a window into pathophysiology that neither tracer alone can provide.

This study also demonstrates the need for caution in interpreting PET data obtained from a single scan. The same pathophysiology can be represented by different metabolic responses depending upon the phase of the disease process at the time of imaging.

DISCLOSURE/CONFLICT OF INTEREST

The authors declare no conflict of interest.

ACKNOWLEDGMENTS

The authors thank S. Jones for help in preparation of the manuscript, RoseAnn Berlin for technical assistance, the NIH, 1P01AI073693-05, and the Lupus Foundation of America, 113121 for support.

REFERENCES

1 Tsokos GC. Systemic lupus erythematosus. *New Engl J Med* 2011; **365**: 2110–2121.
2 The American College of Rheumatology nomenclature and case definitions for neuropsychiatric lupus syndromes. *Arthritis Rheum* 1999; **42**: 599–608.
3 Mackay M, Ulug AM, Volpe BT. Neuropsychiatric systemic lupus erythematosus: mechanisms of injury. In: Lahita RG, Tsokos G, Buyon IP, Koike T (eds). *Systemic Lupus Erythematosus*. Academic Press: London, 2011, pp 491–511.
4 Carbotte RM, Denburg SD, Denburg JA, Nahmias C, Garnett ES. Fluctuating cognitive abnormalities and cerebral glucose metabolism in neuropsychiatric systemic lupus erythematosus. *J Neurol Neurosurg Psychiatry* 1992; **55**: 1054–1059.
5 Kao CH, Ho YJ, Lan JL, Changlai SP, Liao KK, Chieng PU. Discrepancy between regional cerebral blood flow and glucose metabolism of the brain in systemic lupus erythematosus patients with normal brain magnetic resonance imaging findings. *Arthritis Rheum* 1999; **42**: 61–68.
6 Komatsu N, Kodama K, Yamanouchi N, Okada S, Noda S, Nawata Y *et al.* Decreased regional cerebral metabolic rate for glucose in systemic lupus erythematosus patients with psychiatric symptoms. *Eur Neurol* 1999; **42**: 41–48.
7 Lee SW, Park MC, Lee SK, Park YB. The efficacy of brain (18)F-fluorodeoxyglucose positron emission tomography in neuropsychiatric lupus patients with normal brain magnetic resonance imaging findings. *Lupus* 2012; **21**: 1531–1537.
8 Otte A, Weiner SM, Hoegerle S, Wolf R, Juengling FD, Peter HH *et al.* Neuropsychiatric systemic lupus erythematosus before and after immunosuppressive treatment: a FDG PET study. *Lupus* 1998; **7**: 57–59.
9 Weiner SM, Otte A, Schumacher M, Klein R, Gutfleisch J, Brink I *et al.* Diagnosis and monitoring of central nervous system involvement in systemic lupus erythematosus: value of F-18 fluorodeoxyglucose PET. *Ann Rheum Dis* 2000; **59**: 377–385.
10 Appenzeller S, Vasconcelos Faria A, Li LM, Costallat LT, Cendes F. Quantitative magnetic resonance imaging analyses and clinical significance of hyperintense white matter lesions in systemic lupus erythematosus patients. *Ann Neurol.* 2008; **64**: 635–643.
11 Kozora E, Filley CM. Cognitive dysfunction and white matter abnormalities in systemic lupus erythematosus. *J Int Neuropsychol Soc* 2011; **3**: 1–8.
12 Ramage AE, Fox PT, Brey RL, Narayana S, Cykowski MD, Naqibuddin M *et al.* Neuroimaging evidence of white matter inflammation in newly diagnosed systemic lupus erythematosus. *Arthritis Rheum* 2011; **63**: 3048–3057.
13 Luyendijk J, Steens SC, Ouwendijk WJ, Steup-Beekman GM, Bollen EL, van der Grond J *et al.* Neuropsychiatric systemic lupus erythematosus: lessons learned from magnetic resonance imaging. *Arthritis Rheum* 2011; **63**: 722–732.
14 Curiel R, Akin EA, Beaulieu G, DePalma L, Hashefi M. PET/CT imaging in systemic lupus erythematosus. *Ann N Y Acad Sci.* 2011; **1228**: 71–80.
15 DeGiorgio LA, Konstantinov KN, Lee SC, Hardin JA, Volpe BT, Diamond B. A subset of lupus anti-DNA antibodies cross-reacts with the NR2 glutamate receptor in systemic lupus erythematosus. *Nat Med* 2001; **7**: 1189–1193.
16 Kowal C, Degiorgio LA, Lee JY, Edgar MA, Huerta PT, Volpe BT *et al.* Human lupus autoantibodies against NMDA receptors mediate cognitive impairment. *Proc Natl Acad Sci USA* 2006; **103**: 19854–19859.
17 Kowal C, DeGiorgio LA, Nakaoka T, Hetherington H, Huerta PT, Diamond B *et al.* Cognition and immunity; antibody impairs memory. *Immunity* 2004; **21**: 179–188.
18 Putterman C, Diamond B. Immunization with a peptide surrogate for double-stranded DNA (dsDNA) induces autoantibody production and renal immunoglobulin deposition. *J Exp Med* 1998; **188**: 29–38.
19 Faust TW, Chang EH, Kowal C, Berlin R, Gazaryan IG, Bertini E *et al.* Neurotoxic lupus autoantibodies alter brain function through two distinct mechanisms. *Proc Natl Acad Sci USA* 2010; **107**: 18569–18574.
20 Huerta PT, Kowal C, DeGiorgio LA, Volpe BT, Diamond B. Immunity and behavior: antibodies alter emotion. *Proc Natl Acad Sci USA* 2006; **103**: 678–683.
21 Mirrione MM, Schiffer WK, Fowler JS, Alexoff DL, Dewey SL, Tsirka SE. A novel approach for imaging brain-behavior relationships in mice reveals unexpected metabolic patterns during seizures in the absence of tissue plasminogen activator. *NeuroImage.* 2007; **38**: 34–42.
22 Schiffer WK, Mirrione MM, Dewey SL. Optimizing experimental protocols for quantitative behavioral imaging with 18F-FDG in rodents. *J Nucl Med* 2007; **48**: 277–287.
23 Franklin KBJ, Paxinos G. *The Mouse Brain in Stereotaxic Coordinates*. 3rd edn, Academic Publishers: San Diego, 2007.
24 Sawiak SJ, Wood NI, Williams GB, Morton AJ, Carpenter TA. Voxel-based morphometry in the R6/2 transgenic mouse reveals differences between genotypes not seen with manual 2D morphometry. *Neurobiol Dis.* 2009; **33**: 20–27.
25 Ma Y, Hof PR, Grant SC, Blackband SJ, Bennett R, Slatest L *et al.* A three-dimensional digital atlas database of the adult C57BL/6J mouse brain by magnetic resonance microscopy. *Neuroscience* 2005; **135**: 1203–1215.

26 Ulug AM, Vo A, Argyelan M, Tanabe L, Schiffer WK, Dewey S *et al.* Cerebellothalamocortical pathway abnormalities in torsinA DYT1 knock-in mice. *Proc Natl Acad Sci USA* 2011; **108**: 6638–6643.
27 Deacon RM, Croucher A, Rawlins JN. Hippocampal cytotoxic lesion effects on species-typical behaviours in mice. *Behav Brain Res* 2002; **132**: 203–213.
28 Laflamme N, Soucy G, Rivest S. Circulating cell wall components derived from gram-negative, not gram-positive, bacteria cause a profound induction of the gene-encoding Toll-like receptor 2 in the CNS. *J Neurochem.* 2001; **79**: 648–657.
29 DiFrancesco MW, Holland SK, Ris MD, Adler CM, Nelson S, DelBello MP *et al.* Functional magnetic resonance imaging assessment of cognitive function in childhood-onset systemic lupus erythematosus: a pilot study. *Arthritis Rheum* 2007; **56**: 4151–4163.
30 Fitzgibbon BM, Fairhall SL, Kirk IJ, Kalev-Zylinska M, Pui K, Dalbeth N *et al.* Functional MRI in NPSLE patients reveals increased parietal and frontal brain activation during a working memory task compared with controls. *Rheumatology* 2008; **47**: 50–53.
31 Mackay M, Bussa MP, Aranow C, Ulug AM, Volpe BT, Huerta PT *et al.* Differences in regional brain activation patterns assessed by functional magnetic resonance imaging in patients with systemic lupus erythematosus stratified by disease duration. *Mol Med* 2011; **17**: 1349–1356.
32 Rocca MA, Agosta F, Mezzapesa DM, Ciboddo G, Falini A, Comi G *et al.* An fMRI study of the motor system in patients with neuropsychiatric systemic lupus erythematosus. *NeuroImage.* 2006; **30**: 478–484.